Supporting Information

Mori et al. 10.1073/pnas.0901269106

SI Materials and Methods

shRNA Against MMP14. Lentiviral plasmids containing shRNA (Mission shRNA; Sigma) against mouse MMP14 were transfected into HEK293 cells using FuGene6 (Roche). Transfected cells were cultured in DMEM containing 5% FBS, 100 U/mL penicillin, and 100 μg/mL streptomycin. Lentivirus was concentrated from filtered culture media (0.45-μm filters) by ultracentrifugation at 25,000 rpm for 90 min. To infect EpH4 cells, 1.0×10^5 cells were plated in each well of a 6-well plate, infected with the lentivirus, treated with polybrene for 30 min, and selected over 4 d with 3 μg/mL puromycin.

Immunofluorescence Analysis of E-Cadherin and Cleaved Caspase-3. Samples were washed in PBS solution and fixed in 4% paraformaldehyde for 15 min at room temperature, permeabilized 3 times for 5 min in 0.5% Igepal Ca-630, and incubated in 0.1% Triton X-100 in PBS solution for 15 min. Samples were blocked overnight at 4 °C in 10% goat serum in PBS solution (PBS-S), and incubated overnight at 4 °C in primary antibody recognizing E-cadherin (Cell Signaling Technology) or cleaved caspase-3 (Cell Signaling Technology) accordingly, at 1:100 dilution in PBS-S. Samples were washed extensively with PBS solution and incubated in secondary antibody at 1:1,000 in PBS-S overnight at 4 °C. Frequency maps of the proteins were constructed from fluorescence images as described in the main text.

EdU Proliferation Assay. Proliferating cells were visualized by using the Click-iT EdU Imaging Kit (Invitrogen). Samples were incubated for 20 h (starting 4 h after micro-patterning) in 10 μM 5-ethynyl-2-deoxyuridine (EdU). They were subsequently fixed in 4% paraformaldehyde for 15 min at room temperature and permeabilized for 15 min in 0.1% Triton X-100 in PBS solution. EdU incorporation was detected by incubation in the Click-iT reaction mixture (as prescribed by the kit) at room temperature. The samples were then washed 3 times for 5 min in PBS solution. Frequency maps of the cell proliferation were constructed from fluorescence images as described in the main text.

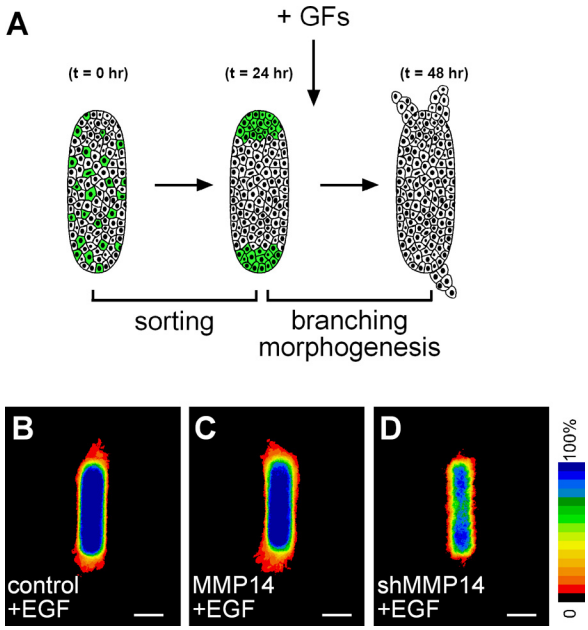

Fig. S1. Engineered tissue model to study cell sorting and morphogenesis. (*A*) Schematic of engineered tissue model. Branching morphogenesis of engineered tissues requires expression of MMP14. Shown are quantification of branching from 50 tubules of control cells (*B*), MMP14-overexpressing cells (*C*), and cells treated with shRNA against MMP14 (*shMMP14*) (*D*). (Scale bars, 50 μm.)

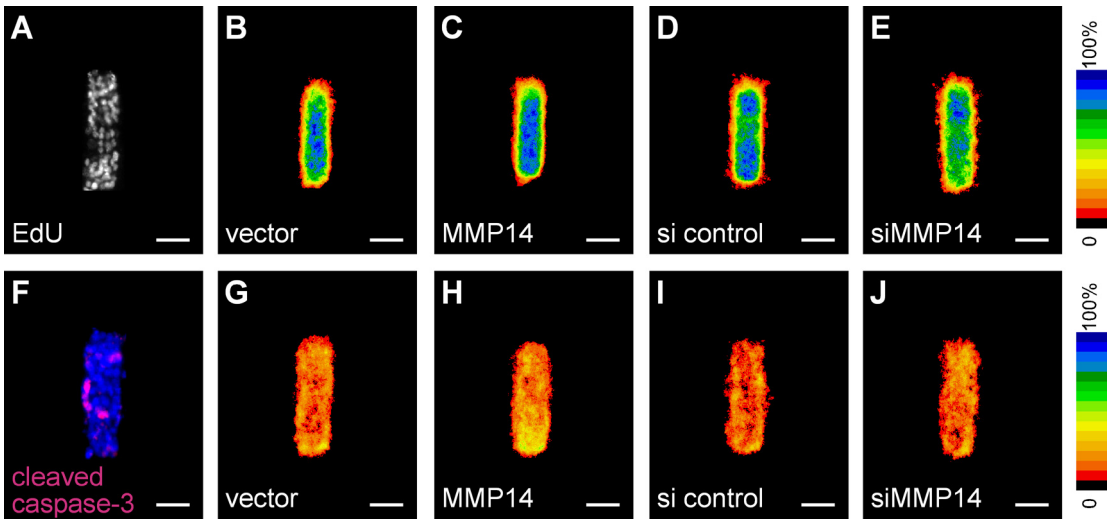

Fig. S2. Mosaic expression of MMP14 does not affect proliferation or apoptosis in the tubules. Immunofluorescence analysis of EdU incorporation in 1 tubule (*A*) and quantification of EdU incorporation in 50 tubules mosaic for vector control (*B*), MMP14(*C*), siRNA control (*si control*) (*D*), or siMMP14 (*E*). Immunofluorescence analysis of cleaved caspase-3 in 1 tubule (*F*) and quantification of cleaved caspase-3 in 50 tubules mosaic for vector control (*G*), MMP14 (*H*), siRNA control (*si control*) (*I*), or siMMP14 (*J*). (Scale bars, 50 μm.)

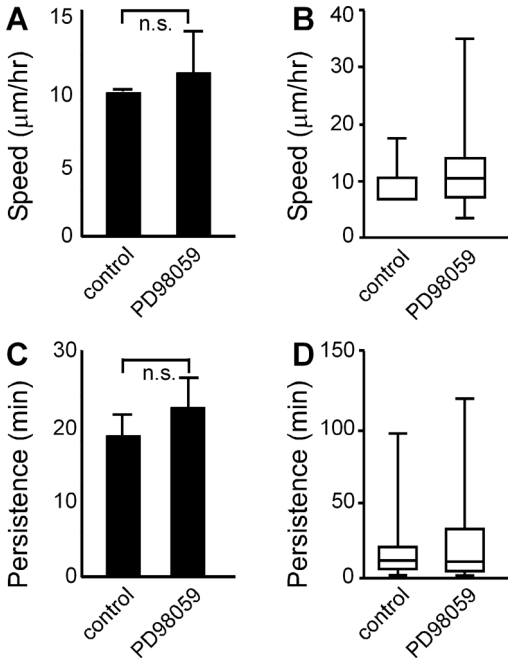

Fig. S3. Inhibition of Erk does not affect cell motility. (*A*) Average speed of individual control cells and cells treated with the MEK inhibitor PD98059. (*B*) Cumulative distribution of cell speed among populations in *A*. (*C*) Persistence time of control cells and cells treated with the MEK inhibitor PD98059. (*D*) Distribution of persistence time amongst populations in *C*. For *A* and *C*, error bars indicate SEM. For *B* and *D*, edges represent 25th and 75th percentiles and error bars represent 10th and 90th percentiles. *n.s.*, not significantly different as determined by *t* test.

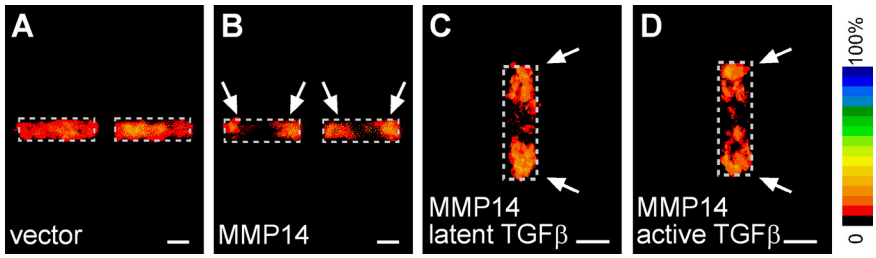

Fig. S4. Self-organization of MMP14 mosaic tubules is not affected by TGF-β gradient. We showed previously that the position of branches was dependent on a gradient in concentration of TGF-β (27). However, endogenous gradient of TGF-β has no effect on sorting, as demonstrated by frequency maps of YFP-expressing cells co-transfected with vector (*A*) and MMP14 (*B*), and constructed into tubules, which increase the local concentration of TGF-β. Exogenous expression of TGF-β also has no effect on sorting, as demonstrated by frequency maps of YFP-expressing cells co-transfected with MMP14 and latent TGF-β1 (C) or active TGF-β1 (D). (Scale bars, 50 μm.)

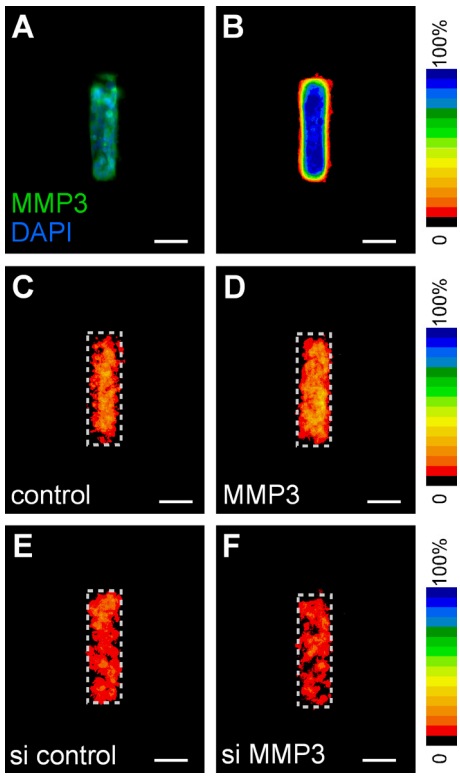

Fig. S5. Tubules mosaic for MMP3 do not sort. Immunofluorescence analysis of MMP3 in 1 tubule (*A*) and quantification of immunofluorescence intensity from 50 tubules (*B*), represented as a frequency map. Frequency map quantifying location of labeled cells co-expressing control vector (*C*) and MMP3 (*D*). Frequency map quantifying location of YFP-expressing cells co-transfected with control siRNA (*si control*) (*E*) and siRNA against MMP3 (*siMMP3*) (*F*). (Scale bars, 50 μm.)

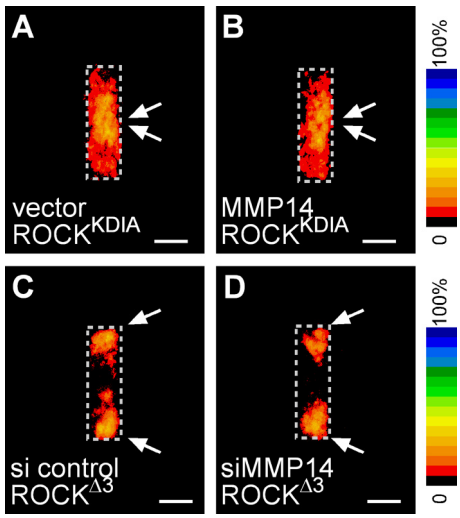

Fig. S6. MMP14-mediated self-organization depends on activated ROCK. Frequency maps quantifying location of YFP-expressing cells co-transfected with dominant negative $ROCK^{KDIA}$ and vector (*A*) and MMP14 (*B*), or co-transfected with constitutively active $ROCK^{\Delta 3}$ and siRNA control (*si control*) (*C*) and siMMP14 (*D*). (Scale bars, 50 μm.)

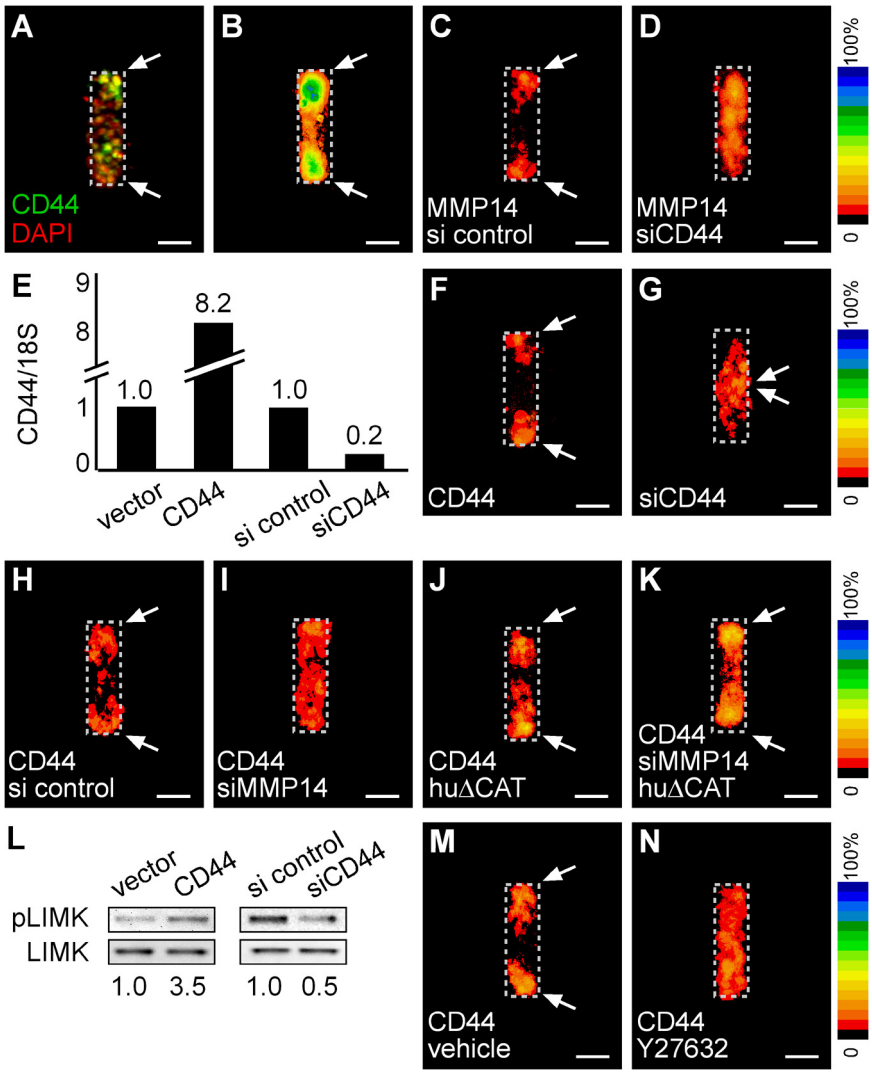

Fig. S7. MMP14-mediated self-organization requires CD44. Immunofluorescence analysis of CD44 in one tubule (*A*) and quantification of immunofluorescence intensity from 50 tubules (*B*). Frequency maps quantifying location of YFP-expressing cells co-transfected with MMP14 and siRNA control (*si control*) (*C*) or siRNA against CD44 (*siCD44*) (*D*). (*E*) Quantitative RT/PCR analysis for CD44 expression in cells transfected with control vector, CD44, siRNA control (*si control*), and siCD44, normalized to levels of 18S rRNA. Frequency maps quantifying location of YFP-expressing cells co-transfected with CD44 (*F*) and siCD44 (*G*) demonstrate that CD44 expression phenocopies MMP14 sorting. CD44-induced self-organization requires expression of the MMP14 hemopexin domain, as demonstrated by frequency maps of YFP-expressing cells co-transfected with CD44 and siRNA control (*si control*) (*H*), siMMP14 (*I*), human MMP14 deleted of the catalytic domain (*huΔCAT*) (*J*), and siMMP14 plus huΔCAT (*K*). CD44 expression activates ROCK signaling, as shown in Western blots for phosphorylated LIMK (*pLIMK*) (*L*) and total LIMK. CD44-induced self-organization requires activation of ROCK, as demonstrated by frequency maps of YFP-expressing cells co-transfected with CD44 and treated with vehicle (*M*) or Y27632 (10 μM) (*N*). (Scale bars, 50 μm.)

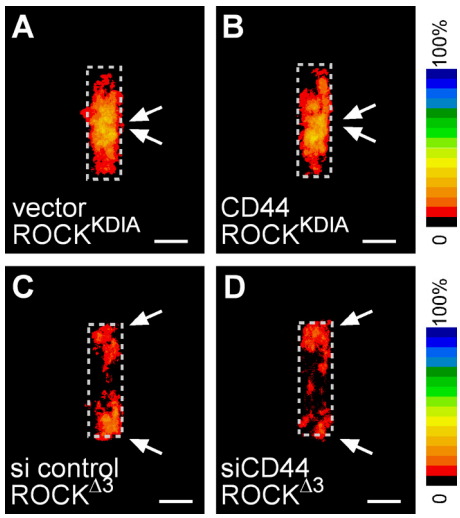

Fig. S8. CD44-mediated self-organization depends on active ROCK. Frequency maps quantifying location of YFP-expressing cells co-transfected with dominant negative $ROCK^{KDIA}$ and vector (*A*) and CD44 (*B*), or co-transfected with constitutively active $ROCK^{\Delta 3}$ and control siRNA (*si control*) (*C*) and siRNA against CD44 (*siCD44*) (*D*). (Scale bars, 50 μm.)

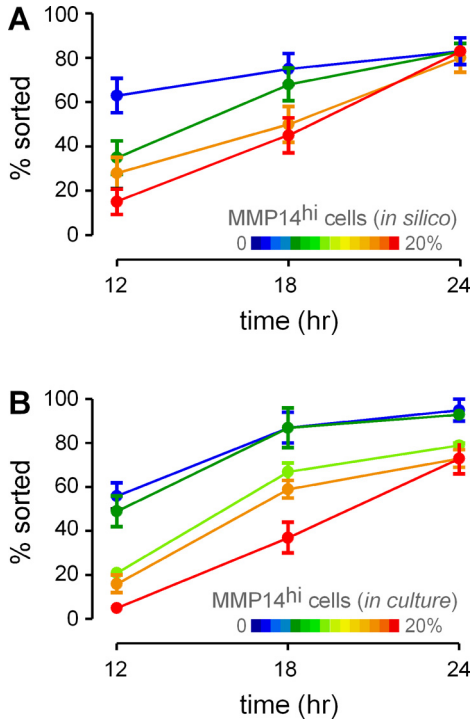

Fig. S9. Increasing initial number of MMP14^{hi} cells per tissue affects kinetics of sorting. (*A*) Average percentage of sorted simulated tissues as a function of time. Each curve represents data from 40 simulated tissues with a different number of MMP14^{hi} cells. Shown are mean values ± SEM. (*B*) Experimental validation of simulation results, represented as percentage of sorted tissues as a function of time. Shown are means ± SEM for 3 independent experiments.

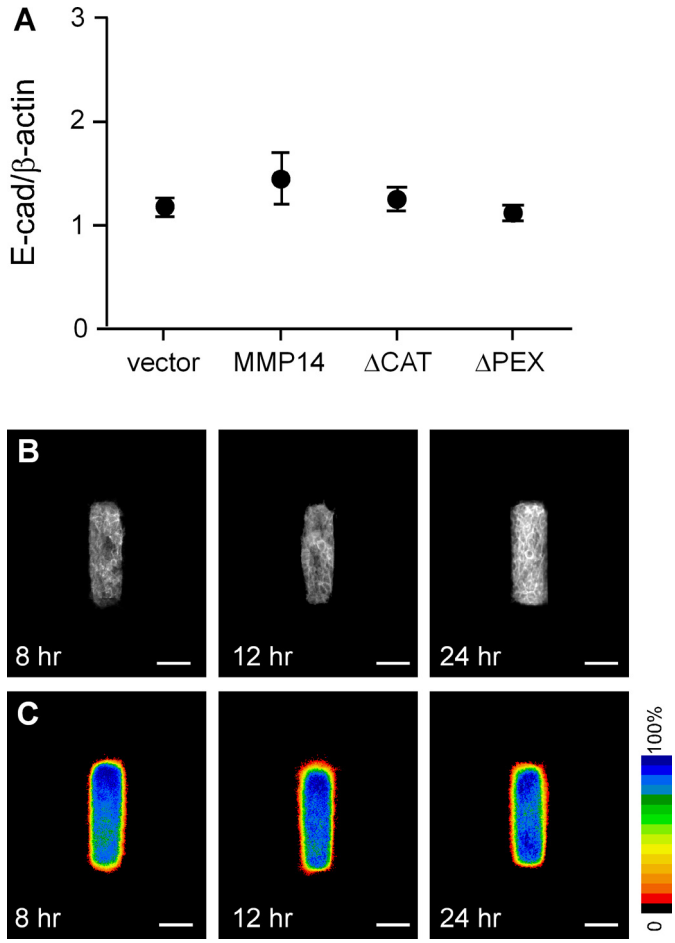

Fig. S10. Expression of MMP14 does not affect expression or distribution of E-cadherin. (*A*) Quantitative RT/PCR analysis for E-cadherin expression in cells transfected with control vector, MMP14, ΔCAT, or ΔPEX, normalized to levels of β-actin. Shown are means ± SEM for 6 experiments. (*B*) Immunofluorescence analysis of E-cadherin in tubules at 8-, 12-, and 24-h time points. (*C*) Frequency maps of E-cadherin staining at 8-, 12-, and 24-h time points. (Scale bars, 50 μm.)